International Journal of
Mathematical Modelling & Computations
Vol. 12, No. 02, Spring 2022, 89- 100

EMHD of Carbon-based Nanofluids over a Plane Sheet with Rotation and Sorret Effect

A. W. Aetdene[a,*], M. Rabiu[b], K. Nantomah[a] and C. Etwire[a]

[a] *Department of Mathematics, CK Tedam University of Technology and Applied Sciences, School of Mathemaical sciences, Navrongo,*
[b] *Department of Physics, University for Development Studies, School of Engineering, Nyanpkala Campus.*

Abstract. In this paper, electro-magneto-hydrodynamic flow of carbon-based nanofluids over a plane sheet is investigated. Carbon nanotubes, graphene and graphite nanonparticles are considered with water as the base fluid. The governing equations formulated for the nanofluids are reduced to nonlinear ordinary differential equations by using similarity transformations. The coupled nonlinear equations are solved numerically by forth order Runge-Kutta method coupled with shooting techique. The numerical results obtained for the skin friction coefficent, nusselt number and sherwood number, as well as the velocity, temperature and concentration profiles for different values of various parameters demonstrate good agreement with literature. The enhanced thermal transport in graphene makes it a good coolant as compared to carbon nanotubes and graphite nanofluids.

Received: 15 May 2021, Revised: 08 February 2022, Accepted: 19 February 2022.

Keywords: EMHD; Nanofluids; Nanoparticle; Similarity transformation; Thermal conductivity; Soret effect.

Index to information contained in this paper

1. Introduction

Electro-magneto-hydrodynamics (EMHD) involves the study of magnetic properties and the behaviour of electrical conducting fluids. A nanofluid exposed to electrical and magnetic fields can have enhanced thermal transport properties [2, 6, 9, 19]. The use of magnetic field for influencing heat generation and absorption process of electrical conducting fluids has many applications in engineering [1, 3, 8, 18, 20]. For example, in metallurgical process, continuous strips or filaments are cooled by drawning the filaments through a quescent fluid. The desired property of the

*Corresponding author. Email: aberezaaya@yahoo.com

Nu	Nusselt Number	Ω	Angular velocity	f	fluid
Le	Lewis Number	μ	Dynamic viscosity	nf	nanofluid
C_f	Skin friction coefficent	θ	Temperature	s	solid
Nt	Thermophoretic number	k	Rotation parameter	CNT	carbon-nanotube
Nb	Brownian number	h	Heat convection	Ref.	Reference
M	Magnetic parameter	ε	Stretching rate	Pres.	Present
EI	Electric parameter				
Sr	Soret number				
Rd	Radiation parameter				
Pr	Prandtl number				
Sh	Sherwood number				

end product which depends on the cooling rate, is then controlled by using an electrically conducting fluid upon application of magnetic field. In an attempt to investigate the cooling properties of carbon nanotubes-water nanofluid, graphene-water nanofluid and graphite-water nanofluid. Three dimentional rotation flow of carbon nanotubes with Darcy-Forchheimer porous medium was examined by authors in refs. [10–12]. They observed that heat transfer rate; local nusselt number, is enhanced for higher volume fractions but reduced for large porosity and further shows a reduction in velocity profiles. However, the opposite was noticed in the temperature profile. The impact of thermal radiation on EMHD flow of carbon nanotubes over a streching sheet was investigated by [17] using homotopy analysis. They found that large values of magnetic field reduce the velocity and temperature profiles, while an increase in velocity was noticed for higher electric parameter. The authors in ref. [15] studied, the three dimensional boundary flow of vescoelastic nanofluid with soret and Dofour effects. They observed that temperature field is improved for large Brownain motion parameter.

In ref [5, 7, 16], the authors investigated the impact of thermal radiation on electrical MHD flow of nanofluid over nonlinear stretching sheet with variable thickness they found out that friction, the rate of heat and mass transfer reduced with an expanding wall thickness. Electric field also enhances the nanofluid velocity and temperature but reduces the concentration. Also, thermal radiation was sensitive to an increase in the nanofluid temperature. Cattaneo-Christov heat flux model for rotating flow and heat transfer of upper-convected Maxwell fluid was investigated [14]. The study revealed that fluid velocity is inversely proportional to the viscoelastic fluid parameter. Numerical simulation of a thermo-electromagneto-hydrodynamic problem in an induction heating furnace was examined [4]. Continuing this study, an investigation of the rotating flow of carbon nanotubes over a stretching sheet with the impact of non-linear thermal radiation and heat generation and absorption was conducted [13]. The results from both studies were quite similar. Howerver, rotation was found to influence thermal transport properties quite substantially.

Inspired by the above existing literature, we conduct an investigation of EMHD flow of carbon-based nanofluids over a linearly streching plane sheet. We will examine the sorret effect, and effects of other parameters on the thermal transport properties of the carbon-based nanofluids.

2. Problem formulation

Consider a three dimensional flow of a carbon-based nanofluid over a rotating plane sheet with angular velocity, Ω. The cartesian coordinate system is such that the plane sheet is aligned with the xy-plane and the nanofluid is located at $z > 0$. Here, water is used as base fluid, and the heat transfer mechanisms modelled are; con-

duction, convection and thermal radiation. A uniform perpenduclar magnetic field B_0 and parallel electric E_0 are applied. From the foregoing, and using the notations spelt out in the numenclature, the principal equations governing the staedy-state flow of the nanofluid velocity, energy and concentration fields are expressed as;

$$\frac{\partial u}{\partial x}+\frac{\partial v}{\partial y}+\frac{\partial w}{\partial z}=0 \tag{1}$$

$$u\frac{\partial u}{\partial x}+v\frac{\partial u}{\partial y}+w\frac{\partial u}{\partial z}-2\Omega v=\frac{\mu_{nf}}{\rho_{nf}}u_{zz}-\frac{\sigma_{nf}B_0}{\rho_{nf}}(B_0u+E_0) \tag{2}$$

$$u\frac{\partial v}{\partial x}+v\frac{\partial v}{\partial y}+w\frac{\partial v}{\partial z}-2\Omega u=\frac{\mu_{nf}}{\rho_{nf}}u_{zz}-\frac{\sigma_{nf}B_0}{\rho_{nf}}(B_0v+E_0) \tag{3}$$

$$\begin{aligned}u\frac{\partial T}{\partial x}+v\frac{\partial T}{\partial y}+w\frac{\partial T}{\partial z}=\frac{k}{\rho c_p}\left(\frac{\partial^2T}{\partial x^2}+\frac{\partial^2T}{\partial y^2}+\frac{\partial^2T}{\partial z^2}\right)+\frac{\mu}{\rho c_p}\left(\frac{\partial u}{\partial y}+\frac{\partial u}{\partial x}+\frac{\partial u}{\partial z}\right)^2\\ +\left(\frac{\partial C}{\partial x}\frac{\partial T}{\partial x}+\frac{\partial C}{\partial y}\frac{\partial T}{\partial y}+\frac{\partial C}{\partial z}\frac{\partial T}{\partial z}\right)-\frac{(q_z(red))}{(\rho C_P)}\end{aligned} \tag{4}$$

$$u\frac{\partial C}{\partial x}+v\frac{\partial C}{\partial y}+w\frac{\partial C}{\partial z}=D_b\left(\frac{\partial^2C}{\partial x^2}+\frac{\partial^2C}{\partial y^2}+\frac{\partial^2C}{\partial z^2}\right)+\frac{D_t}{T_\infty}\left(\frac{\partial^2T}{\partial x^2}+\frac{\partial^2T}{\partial y^2}+\frac{\partial^2T}{\partial z^2}\right) \tag{5}$$

The associated boundary conditions of the problem can be written as;

$$\begin{cases}u=u_w=\varepsilon x;\ v=w=0,\ C=C_f;\ -k_{nf}\frac{\partial T}{\partial z}=h_f(T_f-T); & z=0\\ u\to 0;\ v\to 0;\ w\to 0;\ T\to\infty;\ C\to C_\infty & z\to\infty\end{cases} \tag{6}$$

In which; u,v,w, T_f and C_f are the velocity components (in x, y, and z directions), base fluid temperature and concentration of the sheet, respectively. T_∞ and C_∞ are the temparature and concentration of nanofluids far away from the sheet. ρ_{nf},μ_{nf} and σ_{nf} represent the density, dynamic viscosity and electrical conductivity. D_b, D_t, k_{nf} and $(\rho c_p)_{nf}$ are the Brownian diffusion coefficient, thermophoresis diffusion coefficient, thermal conductivity and specific heat capacity of the nanoparticles, respectively. The radiation term, q^{rad} is defined based on Roseland approximation as $q^{rad}=\frac{\partial T^4}{\partial z}$. Using Taylor's expansion series and ignoring higher terms, the expression can be written as; $q^{rad}=T^3\frac{\partial T}{\partial z}$. The dimensionless numbers; $Pr=\frac{(\rho c_p)_f}{k_f}$ indecate the prandtl number, $k=\frac{\Omega}{\varepsilon}$ represent the rotation parameter, $EI=\frac{E_0}{\varepsilon x^2B_0}$ is the electric parameter, $M=\frac{\sigma_{nf}B_0^2}{\varepsilon}$ is the magnetic parameter, $Le=\frac{\varepsilon}{D_b}$ is the Lowis number, $Nb=\mu D_b(\frac{C_f-C_\infty}{\nu_f})$ is the Brownian diffusion parameter, $Nt=\frac{D_t(T_f-T_\infty)}{T_\infty}$ is the thermophoresis parameter and $Sr=\frac{D_k(T_f-T_\infty)}{T(C_f-C_\infty)}$ is the soret number. The mathematical relations of the nanofluid parameters, as in [17] and [21] are;

$$\nu_f = \frac{\mu_f}{\rho_f}, \quad \rho_{nf} = (1-\varphi)\rho_f + \varphi\rho_s, \quad \alpha_{nf} = \frac{k_{nf}}{(\rho c_p)_{nf}} \tag{7}$$

$$\mu_{nf} = \frac{\mu_f}{(1-\phi)^{2.5}}, \quad (\rho c_p)_{nf} = (1-\phi)(c_p)_f + \varphi(c_p)_s \tag{8}$$

$$\frac{\sigma_{nf}}{\sigma_f} = 1 + \frac{3\varphi(\sigma_s - \sigma_f)}{(\sigma_s - 2\sigma_f) - (\sigma_s - \sigma_f)\varphi} \tag{9}$$

$$\frac{k_{nf}}{k_f} = \frac{1-\varphi+2\varphi(\frac{k_s}{k_s-k_f} ln\frac{k_s+k_f}{2k_f})}{1-\phi+2\varphi(\frac{k_s}{k_s-k_f} ln\frac{k_s+k_f}{2k_f})} \tag{10}$$

In the above relations; ν_f, μ_f, ρ_f and k_f are the kinematic viscosity, dynamic viscosity, density and thermal conductivity of the base fluid, respectively. $\rho_s, k_s, (c_p)_s$ are the density, thermal conductivity and heat capacitance of the nanoparticles, respectively; α is the solid volume fraction of the nanoparticles.
By using the following similarity transformations;

$$u = \varepsilon x f'(\eta),\ v = \varepsilon x g(\eta),\ w = -\sqrt{\varepsilon v_f f(\eta)}, \tag{11}$$

$$\theta(\eta) = \frac{T - T_\infty}{T_f - T_\infty},\ \phi(\eta) = \frac{C - C_\infty}{C_f - C_\infty}, \tag{12}$$

$$\eta = z\left[\frac{\varepsilon}{v_f}\right]^{\frac{1}{2}}, \tag{13}$$

and applying the above transformations, the continuity equation is automatically satisfied. The remaining equations (1-5) are then reduced to nonlinear ordinary differential equations (ODEs);

$$f'''(\eta) - (1-\varphi)^{2.5}\left((1-\eta) + \frac{\rho_s}{\rho_f}\varphi\right) f(\eta)f''(\eta) - (f'(\eta))^2 + 2kg(\eta) - \frac{\sigma_{nf}}{\sigma_f}(Mf'(\eta) + EI) = 0. \tag{14}$$

$$g''(\eta) - (1-\varphi)^{2.5}\left((1-\eta) + \frac{\rho_s}{\rho_f}\varphi\right) f(\eta)g'(\eta) + f'(\eta)g(\eta) - 2kf'(\eta) - \frac{\sigma_{nf}}{\sigma_f}(Mg(\eta) + EI) = 0, \tag{15}$$

$$\frac{1}{Pr}\left(\frac{k_{nf}}{k_f} + \frac{4}{3}Rd\right)\theta''(\eta) + ((1-\varphi) + \frac{(c_p)_s}{(c_p)_f})[f(\eta)\theta'(\eta) - N_b\varphi'(\eta)\theta'(\eta)] = 0, \tag{16}$$

$$\phi''(\eta) + Lef(\eta)\phi'(\eta) - Pr\frac{N_t}{N_b}\theta''(\eta) - Sr = 0. \tag{17}$$

Similarly, the transformed boundary conditions becomes;

$$\begin{cases} f(\eta) = g(\eta) = 0;\ \phi(\eta) = 1;\ f'(\eta) = 1;\ \theta'(\eta) = \frac{k_f}{k_{nf}}(1 - \theta(\eta))\lambda; & \eta = 0 \\ f(\eta) \to 0;\ g(\eta) \to 0; & \eta \to \infty \end{cases} \tag{18}$$

3. Numerical and graphical results and discussions

In order to solve the above coupled nonlinear ODES using Runge-Kutta and shooting methods, the values for physical properties of the base fluid an nanoparticles are required. Typical values are shown in Table 1 below;

Table 1. Physical properties of water and nanoparticles.

	Base fluid	Nanoparticles			
Property	Water	SWCNTS	Graphene	Graphite	MWCNTS
ρ ($\frac{kg}{m^3}$)	997.1	2600	900	641	1600
k ($\frac{W}{mk}$)	0.613	6600	2000	25-470	3000
c_p ($\frac{J}{kgK}$)	4179	425	710	710-830	796
σ ($\frac{S}{m}$)	0.05	$10^6 - 10^7$	$10^7 - 10^8$	2 - 3 $\times 10^5$	$10^6 - 10^7$

3.1 *Graphical results and discussions*

This part investigates the effects of various parameters, such as; magnetic parameter (M), electric parameter (EI), rotation parameter (k), radiation parameter (Rd), Prandtl number (Pr), volume fraction (φ), Lewis number (Le), Thermophoretic number (N_t), and Brownian number (N_b) on the velocity; $f'(\eta)$ and $g(\eta)$, temperature distribution, $\theta(\eta)$ and concentration profile, $\phi(\eta)$. The numerical results are obtained from three types of nanofluids, namely; graphene-water nanofluid, graphite-water nanofluid and carbon nanotubes-water (CNTS-water) nanofluid.

Figure 1 shows the physical effects of magnetic parameter M on $f(\eta)$ and $g(\eta)$. It is obvious from the plots that, an increase in the magnetic parameter leads to a decrease in the velocity profiles; $f(\eta)$, $g(\eta)$. This is due to the augmented Lorentz force which in turn reduces the velocity of the flow. It is also noted that, CNT-water nanofluids, has the highest velocity followed by graphite-water and grahene-water nanofluids.

The effects of the electric parameter EI on $f(\eta)$ and $g(\eta)$ are depicted in Figure 2. It is clear in both graphs that increasing the electric parameter have influenced in the velocities $f(\eta)$ and $g(\eta)$.This may be due to the fact that, the electric current produces fast ionization in the nanofluid which in turn increases the motion of the nanoparticles. It is observed that, graphene nanofluid has the highest velocity followed by graphite nanofluid and carbon-nanotube nanofluid, respectively. Figure 3 shows the variation of $f(\eta)$ and $g(\eta)$ for dissimilar values of volume fraction parameter. It is clear from the plots that, the increased in volume fraction improves

the energy, reduces intermolecular forces of the nanofluid which leads to increase in the motion of the nanofluid, which also in turns increased the velocity for $f(\eta)$ but does opposite in the transverse velocity $g(\eta)$. Figures 4 illustrate the effects of rotation parameter k on $f'(\eta)$ and $g(\eta)$. It is clear from the plots, higher values of rotation parameter induce lower velocity profile on $f'(\eta)$ and $g(\eta)$,

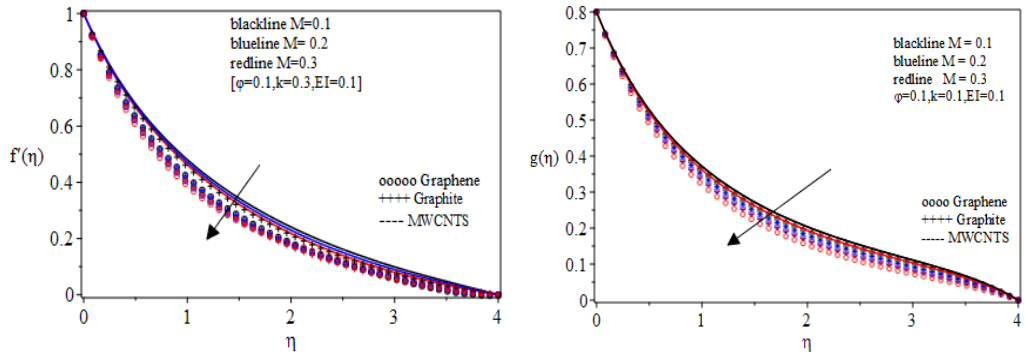

Figure 1. Effect of magnetic parameter on f'(η) and g(η).

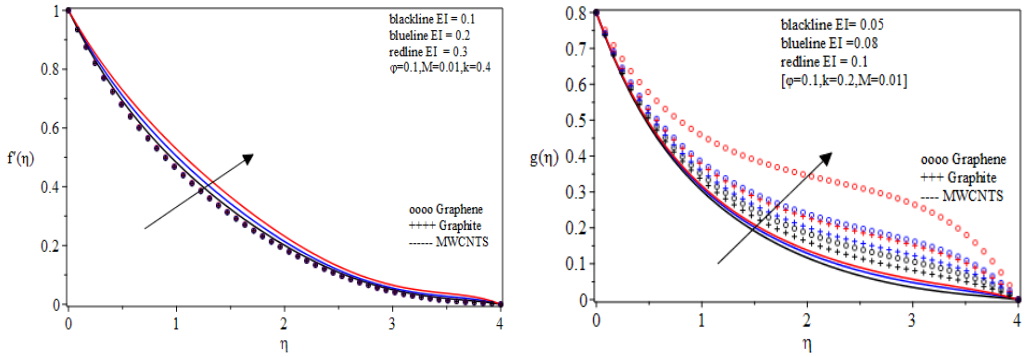

Figure 2. Effect of Electric parameter on f'(η) and g(η).

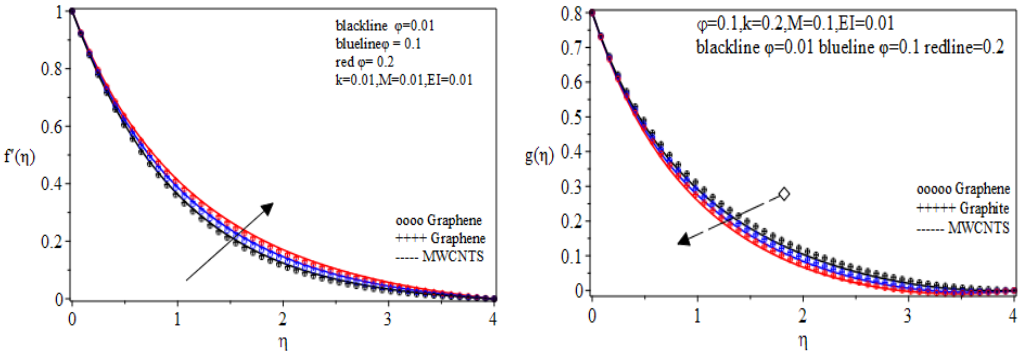

Figure 3. Effect of volume fraction parameter on $f'(\eta)$ and $g(\eta)$.

The effects of Prandtl number and Brownian diffusion parameter on temperature profile are shown in Figure 5 (left). The Prandtl number evaluates the relation of the momentum to the thermal transport ability of a fluid. It is observed from the plots that, higher values of Prandtl number reduces the thermal diffusion across the plane. It is also noted that graphene-water nanofluid is doing well in terms of

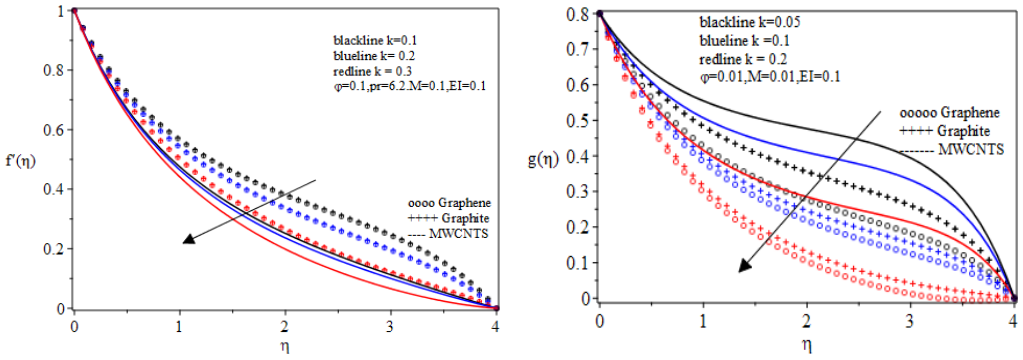

Figure 4. Effect of rotation parameter k on f'(η).

reduction in thermal transport, followed by carbon-nanotubes-water, and graphite-water nanofuids, respectively. Effect of the Brownain diffusion parameter is also exposed in Figure 5 (right). With increased in Brownian parameter implies high random motion of the nanoparticles which in turn increase the temperature due to frequent collisions. In terms of thermal transport enhancement, it is also clear from the figure that, CNTS-water nanofluid is doing well followed by Graphite-water and Graphene-water nanofluids.

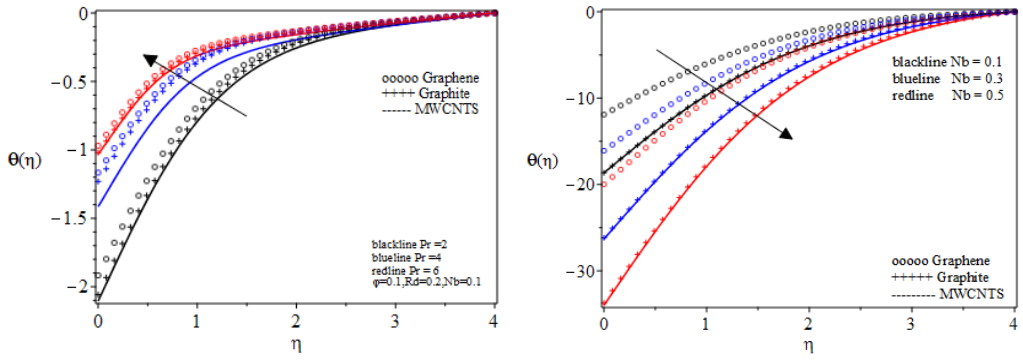

Figure 5. Effects of prantl parameter pr and Browian diffusion Nt on $\theta(\eta)$.

Figure 6 represents the effects of radiation parameter and volume fraction on temperature profile. It is clear from the plot that, higher values of radiation parameter transport more heat to the nanofluid which physically improves cooling of system. More over, the carbon nanotubes are doing well as compare to the rest of the fluid, followed by graphite and graphene respectively. While the temperature profile for different values of volume fraction for carbon natube-water nanofluid, graphene-water and graphite-water display interesting features. It is found out that large nanoparticle volume fraction leads to more heat transport to nanofluid, moreover, graphite-water is performing well as compared the rest, followed by carbon-water and graphene-water nanofluid.

The effects of thermophoretic and Prantl parameters on nanoparticle concentration is illustrated in Figure 7. Here, large values of N_t lead to improvement in thermal conductivity and boundary layer thickness. It is observed that, Grapene nanofluids is performing well as compare to the other nanofluids. Finally, the combined effects of Lewis number and brownian diffusion parameter are shown in Figure 8. The increasing values of Lewis number and Brownian diffusion parametr causes nanoparticle diffusion to take place. This induces a reduction in concentration profile, $\phi(\eta)$.

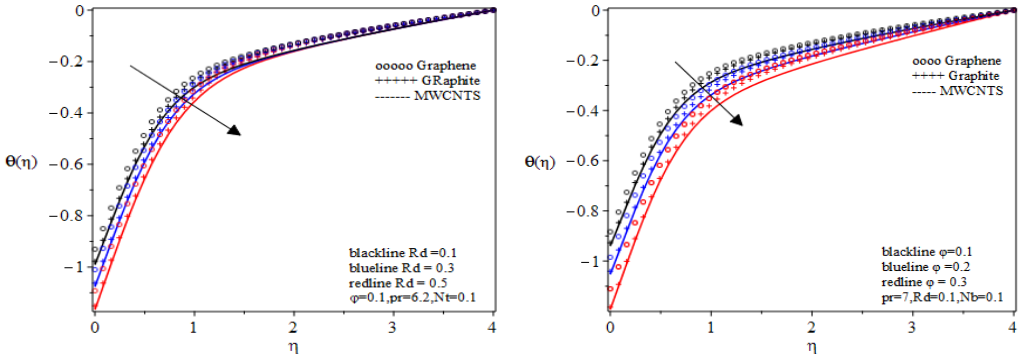

Figure 6. Effects of radiation and volume fraction parameters on $\theta(\eta)$.

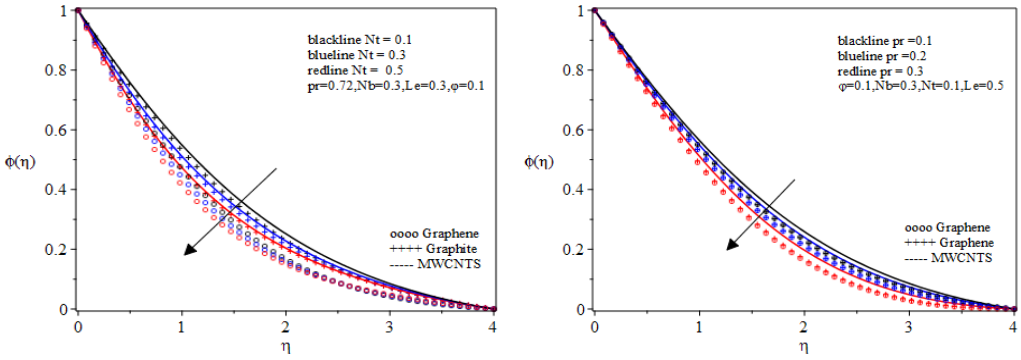

Figure 7. Effects of thermophoresis and prandtl parameters on $\phi(\eta)$.

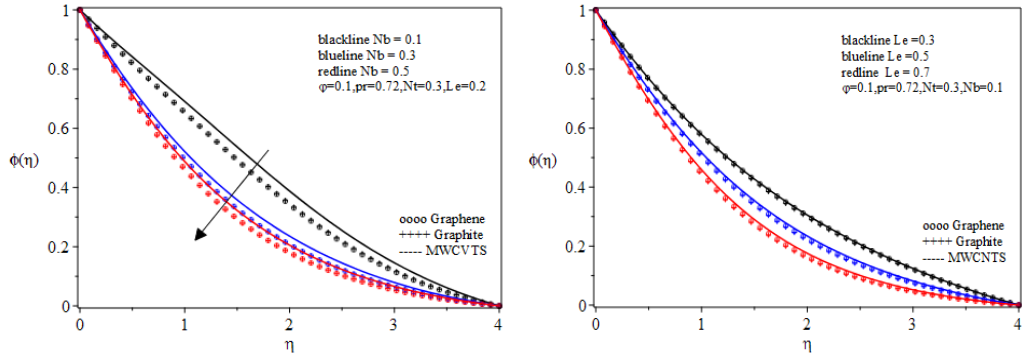

Figure 8. Effects of Brownian diffusion parameter and Lewis number on $\phi(\eta)$.

3.2 *Numerical results and discussions*

Table 2 shows the impact of varying values of Prandtl number on the Nusselt number. It can be seen that the validation of the present results is in excellent agreement with the previous cases studied by Haq et al (2017) and Shah et al (2019) for $\varphi = 0$.

The effects of the Nusselt numer along the horizontal flow direction, for varying values of Pr, Rd, Nb, and φ are displayed numerically in Table 3. Here, we have conpared with only MWCNT-water nanofluid. The numrical results indicate quite good agreement. Both graphene-water and graphite-water nanofluids demonstrate enhanced thermal transfer properties, but graphene-water nanofluid has appreciable good performance compared to the graphite-water nanofluid.

The effects of the skin friction coefficients for varying values of M, EI, k, and φ for MWCNTS-water nanofluid are displayed numerically in Table 4. The influence

Table 2. Impact of Pr on Nusselt Number when $\varphi = 0$.

Pr	Nusselt Number, Nu		
	Ref. results [12]	Ref. results [17]	Present results
0.71	0.470	0.477	0.47000
7.00	1.491	1.522	1.51508
71.00	0.330	0.345	0.33513

Table 3. Comparison of numerical values of local Nusselt numbers for varying values of Pr, Rd, Nb, and φ. Ref. results [17].

				$-Nu_x Re_x^{\frac{1}{2}}$			
				MWCNTS		Graphite	Graphene
Pr	Rd	Nb	φ	Ref. results	Pres. results	Pres. results	Pres. results
0.0	0.1	0.1	0.1	0.11696	0.1111100	0.111111	0.111110
0.3				0.11664	0.1058456	0.109210	0.109275
0.5				0.11695	0.1029026	0.108030	0.108122
0.1	0.0			0.11696	0.1082190	0.110375	0.110402
	0.3			0.11690	0.1100270	0.110583	0.110602
	0.5			0.11695	0.1103257	0.110667	0.110683
	0.1	0.0		0.11845	0.1105375	0.110960	0.110920
		0.3		0.12061	0.1063209	0.109490	0.109516
		0.5		0.12250	0.1034129	0.108853	0.108547
		0.1	0.0	0.11602	0.1091933	0.110447	0.110471
			0.3	0.11694	0.1092984	0.110487	0.110511
			0.5	0.11789	0.1093668	0.110512	0.110537

of varrious values of magnetic parameter, electric parameter, volume fraction and rotation parameter is evident. Higher values of the electric and the rotation parameters induce substantial effects on the skin friction. The values along the transport direction are much affectted.

Table 4. Comparison of numerical values of skin friction coefficent for varying values of M, EI, k, and φ for MWCNT-water nanofluid.

				$-C_{fx} Re_x^{\frac{1}{2}}$		$-C_{fy} Re_x^{\frac{1}{2}}$	
M	EI	k	φ	Ref. results [17]	Pres. results	Ref. results [17]	Pres. results
0.0	0.1	0.1	0.1	1.22193	0.89657	0.30052	0.05756
0.3				1.28770	0.95108	0.29796	0.46598
0.5				1.41138	1.06627	0.29436	0.34039
0.1	0.0			1.31769	0.81328	0.29610	0.28837
	0.3			1.38321	1.12754	0.29582	0.46598
	0.5			1.41495	1.31689	0.29569	0.36857
	0.1	0.0		1.34433	0.94879	0.27033	0.16487
		0.3		1.36884	0.94744	0.32059	0.25395
		0.5		1.39539	1.03569	0.34351	0.49332
		0.1	0.0	1.49690	0.91415	0.26365	0.01662
			0.3	1.23280	0.99833	0.28369	0.02964
			0.5	1.49768	1.18135	0.30225	0.03443

For the cases of graphite-waater and graphene-water nanofluids, the effects of the skin friction coefficients are displayed numerically in Table 5. Similarly, the impact of varrious values of magnetic parameter, electric parameter, volume fraction and rotation parameter is evident. It can seen that higher values of the electric and the rotation parameters cause enhancement in the skin friction values. The situation in MWCNT-water nanofluid is quite similar, as values along the transport direction are much affectted.

Table 6 shows the omparison of numerical values of sherwood number for varying

Table 5. Comparison of numerical values of skin friction coefficent for varying values of M, EI, k, and φ for graphite-water, graphene-water nanofluids

				$-C_{fx}Re_x^{\frac{1}{2}}$		$-C_{fy}Re_x^{\frac{1}{2}}$	
M	EI	k	φ	Graphite	Graphene	Graphite	Graphene
0.0	0.1	0.1	0.1	1.19753	1.15835	0.01531	0.05692
0.3				1.28765	1.70670	0.01421	0.05910
0.5				1.34606	1.17884	0.10135	0.05690
0.1	0.0			1.18303	1.15645	0.63340	0.63320
	0.3			1.13178	1.17865	0.08205	0.04411
	0.5			1.40800	1.18655	0.17932	0.03129
	0.1	0.0		1.12279	1.13769	0.04772	0.06870
		0.3		1.23251	1.20108	0.14002	0.06817
		0.5		1.12431	1.12261	0.26422	0.06825
		0.1	0.0	1.20342	1.16179	0.01555	0.00630
			0.3	1.26583	1.16898	0.01399	0.19532
			0.5	1.29040	1.18135	0.01339	0.20250

values of Pr, Nb, Nt, Le, and Sr for the nanofluids. It can be seen that, higher values of Pr, Nb, Nt and Le leads to decreased in sherwood numbers for MWCNTS and Graphene nanofluids but does the opposite for Graphite nanofluid. While higher values of Sr numbers induced increased in sherwood numbers.

Table 6. Comparison of numerical values of sherwood number for varying values of Pr, Nb, Nt, Le, and Sr for the nanofluids

					$-Sh_x$		
					MWCNT	Graphene	Graphite
Pr	Nb	Nt	Le	Sr	Pres. results	Pres. results	Pres. results
0.9	0.1	0.1	0.1	0.1	0.814522	1.0207030	1.0000000
1.0					0.789240	1.0114924	1.0102970
1.1	0.1				0.722050	1.1624650	1.0001830
	0.2				1.059230	1.0618990	1.0617360
	0.3	0.0			1.052905	1.0619210	1.0617614
		0.9			1.048260	1.0619270	1.0610757
		1,0			1.046582	1.1737717	0.9999900
		1.1	0.0		1.156529	1.1864132	1.1611634
			0.1		1.169073	1.0166240	1.1737717
			0.2		1.012509	1.0166240	1.1864132
			0.3	0.00	1.017514	1.1117026	1.0166240
				0.01	1.502917	1.111713	1.1117026
				0.02	1.507196	1.117264	1.5070295

4. Conclusions

This work investigated EMHD flow of carbon-based nanofluids over a plane sheet. Carbon-nanotubes, graphene and graphite nanoparticles, with water as the base fluid are studied. The governing equations formulated are reduced to nonlinear equations by using similarity transformations. The coulpled nonlinear equations are solved numerically using Runge-Kutta algorithm coupled with Newton-Raphson shooting technique. The velocity, temperature and concentration solutions are demonstrated graphically for wide ranges of Prandtl, Nussel, Sherwood, thermophoretic, Browian numbers, as wel as skin friction coeefient, magnetic parameter, electric parameter and volume fractions. The sorret and magnetic numbers appear to have great influence on the skin friction coeffient and thermal transport properties.

The following major conclusions were observed;

(i) The velocities are slower for higher values of rotation, magnetic and electric parameters.

(ii) Heat transfer rate at the surface of the plate decreases as prandtl number is increased.
(iii) Graphene nanofluid demonstrates highest heat transfer rate as compared to the rest of the nanofluids.
(iv) Increase in radiation parameter also induced more heat transfer to the nanofluid.
(v) The MWCNTS has the highest heat absortion capacity as campared to other nanofluids.
(vi) Increase in volume fraction parameter also leads to increase in heat transfer rate, which inturn reduces heat lost in the system.
(vii) The skin friction coefficient values increase with increased in volume fraction parameter.
(viii) The graphite nanofluid has higher skin friction followed by graphene and MWCNTS, respectively.
(ix) Grahene-water nanofluid exisbits high coolant properties as compared to the graphite and MWCNTS nanofluids.

References

[1] N. Ali, A. M. Bahman, N. F. Aljuwayhel, S. A. Ebrahim, S. Mukherjee and A. Alsayegh, Carbon-Based Nanofluids and Their Advances towards Heat Transfer Applications – A Review, Nanomaterials, **11 (6)** (2021), 1628, doi:10.3390/nano11061628.
[2] R. Azizian, Nanofluids in Electronics Cooling Applications, Advanced Thermal Solutions, Inc., Norwood, MA, (2017).
[3] J. A. Baylis and J. C. R. Hunt, MHD flow in an annular channel; theory and experiment, Journal of Fluid Mechanics, **48 (3)** (1971) 423–428.
[4] A. Bermúdez, D. Gómez, M. Muñiz, P. Salgado and R. Vazquez, Numerical simulation of a thermo-electromagneto-hydrodynamic problem in an induction heating furnace, Applied Numerical Mathematics, **59 (9)** (2009) 2082–2104.
[5] M. Bilal, Micropolar flow of EMHD nanofluid with nonlinear thermal radiation and slip effects, Alexandria Engineering Journal, **59 (2)** (2020) 965–976.
[6] S. U. S. Choi and J. A. Eastman, Enhancing thermal conductivity of fluids with nanoparticles, Argonne National Lab., Illinois, United States, (1995).
[7] Y. S. Daniel, Z. A. Aziz, Z. Ismail and F. Salah, Impact of thermal radiation on electrical MHD ow of nanouid over nonlinear stretching sheet with variable thickness, Alexandria Engineering Journal, **57 (3)** (2018) 2187–2197.
[8] S. K. Das, S. U. Choi and H. E. Patel, Heat transfer in nanofluids – A review, Heat Transfer Engineering, **27 (10)** (2006) 3–19.
[9] S. K. Das, S. U. Choi, W. Yu and T. Pradeep, Nanofluids: Science and Technology, John Wiley and Sons, (2007).
[10] A. Dawar, Z. Shah, W. Khan, M. Idrees and S. Islam, Unsteady squeezing ow of magnetohydrodynamic carbon nanotube nanouid in rotating channels with entropy generation and viscous dissipation, Advances in Mechanical Engineering, **11 (1)** (2019), doi:10.1177/1687814018823100.
[11] R. U. Haq, F. Shahzad and Q. M. Al-Mdallal, MHD pulsatile flow of engine oil based carbon nanotubes between two concentric cylinders, Results in Physics, **7** (2017) 57–68.
[12] T. Hayat, F. Haider, T. Muhammad and A. Alsaedi, Three-dimensional rotating ow of carbon nanotubes with darcy-forchheimer porous medium, PLOS ONE, **12 (7)** (2017), e0179576, doi:10.1371/journal.pone.0179576.
[13] S. Muhammad, G. Ali, Z. Shah, S. Islam and S. A. Hussain, The rotating ow of magneto hydrodynamic carbon nanotubes over a stretching sheet with the impact of non-linear thermal radiation and heat generation/absorption, Applied Sciences, **8 (4)** (2018), 482, doi:10.3390/app8040482.
[14] M. Mustafa, Cattaneo-christov heat ux model for rotating ow and heat transfer of upper-convected maxwell uid, AIP Advances, **5 (4)** (2015) 047109, doi:10.1063/1.4917306.
[15] M. Ramzan, S. Inam and S. Shehzad, Three dimensional boundary layer ow of a viscoelastic nanouid with soret and dufour effects, Alexandria Engineering Journal, **55 (1)** (2016) 311–319.
[16] A. Raptis, C. Perdikis and H. S. Takhar, Effect of thermal radiation on MHD flow, Applied Mathematics and Computation, **153 (3)** (2004) 645–649.
[17] Z. Shah, E. Bonyah, S. Islam and T. Gul, Impact of thermal radiation on electrical MHD rotating ow of carbon nanotubes over a stretching sheet, AIP Advances, **9 (1)** (2019) 015115, doi:10.1063/1.5048078.
[18] E. M. Sparrow and R. D. Cess, The effect of a magnetic field on free convection heat transfer, International Journal of Heat and Mass Transfer, **3 (4)** (1961) 267–274.
[19] M. M. Tawfik, Experimental studies of nanofluid thermal conductivity enhancement and applications: A review, Renewable and Sustainable Energy Reviews, **75** (2017) 1239–1253.
[20] R. Taylor, S. Coulombe, T. Otanicar, P. Phelan, A. Gunawan, W. Lv, G. Rosengarten, R. Prasher

and H. Tyagi, Small particles, big impacts: A review of the diverse applications of nanofluids, Journal of Applied Physics, **113 (1)** (2013) 011301, doi:10.1063/1.4754271.

[21] Y. Yirga and D. Tesfay, Heat and mass transfer in MHD ow of nanouids through a porous media due to a permeable stretching sheet with viscous dissipation and chemical reaction effects, International Journal of Mechanical and Mechatronics Engineering, **9 (5)** (2015) 709–716.